UCSF
UC San Francisco Previously Published Works

Title

Functional connectivity within glioblastoma impacts overall survival

Permalink

https://escholarship.org/uc/item/5d8033qb

Journal

Neuro-Oncology, 23(3)

ISSN

1522-8517

Authors

Daniel, Andy GS
Park, Ki Yun
Roland, Jarod L
et al.

Publication Date

2021-03-25

DOI

10.1093/neuonc/noaa189

Copyright Information

This work is made available under the terms of a Creative Commons Attribution-NonCommercial License, available at https://creativecommons.org/licenses/by-nc/4.0/

Peer reviewed

Neuro-Oncology

Functional connectivity within glioblastoma impacts overall survival

Andy G. S. Daniel, Ki Yun Park, Jarod L. Roland, Donna Dierker, James Gross, Joseph B. Humphries, Carl D. Hacker, Abraham Z. Snyder, Joshua S. Shimony, and Eric C. Leuthardt

Department of Biomedical Engineering, McKelvey School of Engineering, Washington University, St. Louis, Missouri (A.G.S.D., J.B.H., E.C.L.) and Mallinckrodt Institute of Radiology, Washington University School of Medicine, St. Louis, Missouri (K.Y.P., D.D., A.Z.S., J.S.S.), Washington University School of Medicine, St Louis, Missouri; Department of Neurological Surgery, University of California San Francisco, San Francisco, California (J.L.R.); School of Medicine (J.G.), Department of Neurological Surgery (C.D.H., E.C.L.), Department of Neuroscience (E.C.L.), Department of Mechanical Engineering and Materials Science (E.C.L.), Center for Innovation in Neuroscience and Technology (E.C.L.), and Brain Laser Center (E.C.L.), Washington University School of Medicine, St Louis, Missouri

Corresponding Author: Eric C. Leuthardt, MD, Department of Neurosurgery, Washington University in St. Louis School of Medicine, Campus Box 8057, 660 South Euclid, St. Louis, MO 63110 (leuthardte@wustl.edu).

Abstract

Background. Glioblastoma (GBM; World Health Organization grade IV) assumes a variable appearance on MRI owing to heterogeneous proliferation and infiltration of its cells. As a result, the neurovascular units responsible for functional connectivity (FC) may exist within gross tumor boundaries, albeit with altered magnitude. Therefore, we hypothesize that the strength of FC within GBMs is predictive of overall survival.

Methods. We used predefined FC regions of interest (ROIs) in de novo GBM patients to characterize the presence of within-tumor FC observable via resting-state functional MRI and its relationship to survival outcomes.

Results. Fifty-seven GBM patients (mean age, 57.8 ± 13.9 y) were analyzed. Functionally connected voxels, not identifiable on conventional structural images, can be routinely found within the tumor mass and was not significantly correlated to tumor size. In patients with known survival times ($n = 31$), higher intranetwork FC strength within GBM tumors was associated with better overall survival even after accounting for clinical and demographic covariates.

Conclusions. These findings suggest the possibility that functionally intact regions may persist within GBMs and that the extent to which FC is maintained may carry prognostic value and inform treatment planning.

Key Points

1. Functionally connected voxels can be routinely found within GBM tumors.

2. Intratumor connectivity strength is a prognostic marker for overall survival.

Glioblastoma multiforme (GBM) is a highly infiltrative and deadly form of brain cancer.[1,2] Given the heterogeneous nature of this disease, its distribution within brain parenchyma is extremely variable. It is clear that tumor growth results in death of surrounding tissue and displacement of native cells. However, limited evidence suggests that functionally intact brain tissue may be preserved within the tumor boundaries.[3–5] Most of this evidence has been derived by intraoperative direct stimulation of sensorimotor and language areas (ie, eloquent cortex).[3–6] This mode of inquiry neglects cognitive processes such as attention, executive function, and planning, which are not easily assessed in the operating room.[7,8] These functions are relevant to patient outcomes; hence, their neglect during presurgical planning may lead to compromised patient well-being and overall survival.[9–11] Moreover, prior studies of preserved intratumor function have been limited by small sample sizes. Accordingly, drawing population inferences regarding survival in patients with brain tumors in general and GBM in particular has been challenging.

Importance of the Study

Assessment of preserved function within GBM tumors has been limited to observation of overt responses to direct electrical stimulation of "eloquent" cortex. This mode of functional assessment ignores crucial functionality outside the sensorimotor and language systems. Moreover, the heterogeneous nature of GBMs implies that preservation of function within tumor boundaries may vary across patients.

The prognostic significance of such preserved function remains uncertain. Using resting-state functional MRI, we examined the extent to which FC is preserved in GBMs. Our results demonstrate that FC can be identified within most GBM tumors. Additionally, the strength of this connectivity may serve as a biomarker with prognostic significance before surgery or other treatments.

Task-based functional magnetic resonance imaging (T-fMRI) is routinely employed during presurgical planning of tumor resections.[12–14] More recently, resting-state functional MRI (rs-fMRI) has been used as an alternative technique for functional mapping with several advantages over T-fMRI. For instance, rs-fMRI can be acquired in patients who are unable to cooperate with a task, such as young children or patients who are cognitively impaired.[15–17] The rs-fMRI method relies on identification of temporally correlated, intrinsic fluctuations of infra-slow blood-oxygen-level-dependent (BOLD) signals (ie, functional connectivity [FC]). The associated topographies are widely known as resting-state networks (RSNs). RSNs correspond to functional systems instantiating attention, executive control, and episodic memory, in addition to motor and language function.[18] Motor and language maps derived by rs-fMRI have shown good correspondence with results obtained with stimulation mapping and T-fMRI.[19,20] Several rs-fMRI studies have identified network-specific changes in patients with brain tumors, but sample sizes were small and tumor pathologies heterogeneous.[21] The possibility of preserved GBM intratumor function has so far not been addressed using rs-fMRI.

We acquired rs-fMRI in 57 de novo GBM patients prior to surgery and evaluated intratumor FC of several RSNs. We tested the hypothesis that the magnitude of this connectivity is associated with overall survival. Our data show that the strength of intratumor FC is an independent predictor of survival. Thus, rs-fMRI has potential prognostic value in GBM patients.

Materials and Methods

Subjects

Fifty-seven patients with new primary GBM underwent evaluation prior to surgical resection. Patients were recruited from the neurosurgery brain tumor service, initially as part of a National Institutes of Health (NIH)–funded tumor database grant (NIH 5R01NS066905). All aspects of the study were approved by the Washington University in St Louis (WUSTL) institutional review board and the clinical data were retrospectively reviewed. The following inclusion criteria were used: new diagnosis of primary brain tumor; age more than 18 years; and clinical need for an MRI scan, including rs-fMRI as determined by the treating neurosurgeon. Exclusion criteria included prior surgery for brain tumor, inability to have an MRI scan, and referral from an outside institution with an MRI scan performed without rs-fMRI.

For control analyses, clinically healthy adult data ($n = 100$ subjects) were obtained from the Harvard–Massachusetts General Hospital (MGH) Brain Genomics Superstruct Project (GSP). This dataset is described by Yeo et al.[22] Adult participants provided written informed consent in accordance with the guidelines set by the institutional review boards of Harvard University and Partners Healthcare.

MRI Acquisition

Data were acquired using a Siemens 3T Trio or Skyra MRI scanner. Patients were scanned using a standard clinical presurgical tumor protocol. Anatomic imaging included T1-weighted (T1w) magnetization prepared rapid acquisition gradient echo (MPRAGE), T2-weighted (T2w) fast spin echo, fluid attenuated inversion recovery (FLAIR) imaging, and postcontrast T1w fast spin echo in 3 projections. The rs-fMRI was acquired using an echo planar imaging sequence (voxel size = 3 mm cubic; echo time [TE] = 27 ms; repetition time [TR] = 2.2–2.9 s; field of view = 256 mm; flip angle = 90°) for a total of 320 frames. For the GSP subjects, the data were acquired as described by Yeo et al briefly summarized here: the data were collected on Siemens Trio 3T scanners using a 12-channel phased-array head coil.[22] The structural data were acquired using a high-resolution multi-echo T1w MPRAGE sequence. The rs-fMRI was collected using a gradient-echo echo planar imaging sequence (voxel size = 3 mm cubic; TE = 30 ms; TR = 3000 ms; field of view = 216 mm; flip angle = 85°). Two BOLD runs were acquired per subject with 124 frames per run (6.2 min).

MRI Preprocessing

Preprocessing procedures used standard approaches as previously described.[16,19] This included compensation for slice-dependent time shifts, removal of systemic odd-even slice intensity differences due to interleaved acquisition, and rigid body correction for head movement within and across runs. Atlas transformation was achieved by composition of affine transforms connecting the functional imaging volumes with the T2w and T1w structural images, resulting in a volumetric time series in isotropic 3 mm³

atlas space. Additional preprocessing included spatial smoothing (6 mm full-width half-maximum Gaussian blur in each direction), voxelwise removal of linear trends over each run, and temporal low pass filtering retaining frequencies less than 0.1 Hz. Spurious variance was reduced by regression of nuisance waveforms derived from head motion correction and extraction of the time series from regions of white matter and cerebrospinal fluid. The whole-brain (global) signal was included as a nuisance regressor. Frame censoring was performed to minimize the impact of head motion on the correlation results. Thus, frames (volumes) in which the root mean square (evaluated over the whole brain) change in voxel intensity relative to the previous frame exceeded 0.5% (relative to the whole-brain mean) were excluded from the FC computations.

Tumor Segmentation

Using the software application ITK-SNAP,[23] brain tumors were segmented semi-automatically using multimodal image acquisitions (T1w, postcontrast T1w, T2w, and FLAIR). This enabled the separation of contrast-enhancing tumor, necrosis, and surrounding FLAIR hyperintense edematous areas from normal cortical and subcortical tissue. Tumor was defined as a contrast-enhancing plus necrotic-appearing region.

Resting-State Network Identification

Based on the study by Hacker et al,[24] 169 ROIs throughout the brain were selected, with each ROI belonging to one of 7 canonical resting-state networks. Using the segmented contrast-enhanced (CE) bounded tumor and the peritumor FLAIR hyperintense "edema" regions as masks, the ROIs found within those areas were identified (Fig. 1C). To create a time series for each resting-state network, the voxels within each network-specific ROI outside of the tumor and peritumor regions (ie, extratumor regions) were averaged together. Using Pearson correlation, the network BOLD time series were then correlated with their corresponding network ROIs found within the tumor to obtain the intranetwork connectivity strength for that ROI. Additionally, the BOLD time series of each network was Pearson correlated with the time series for each voxel found within the tumor (ie, intratumor) to identify the correlation strength of each voxel to every network. Computed correlations were Fisher z-transformed. A conservative threshold of $r > 0.3$ was taken as indicating the presence of FC of a voxel to a particular network.[25] Each of the 100 controls in the GSP dataset was treated identically to every GBM patient. Patient-derived tumor and peritumor masks were used to create virtual tumor and peritumor regions. Seed-based FC then was computed in each control.

Statistical Analysis

Statistical analyses were performed in Excel, R, GraphPad Prism, and MatLab. The log-rank test was used to compare Kaplan–Meier survival curves of intratumor connectivity
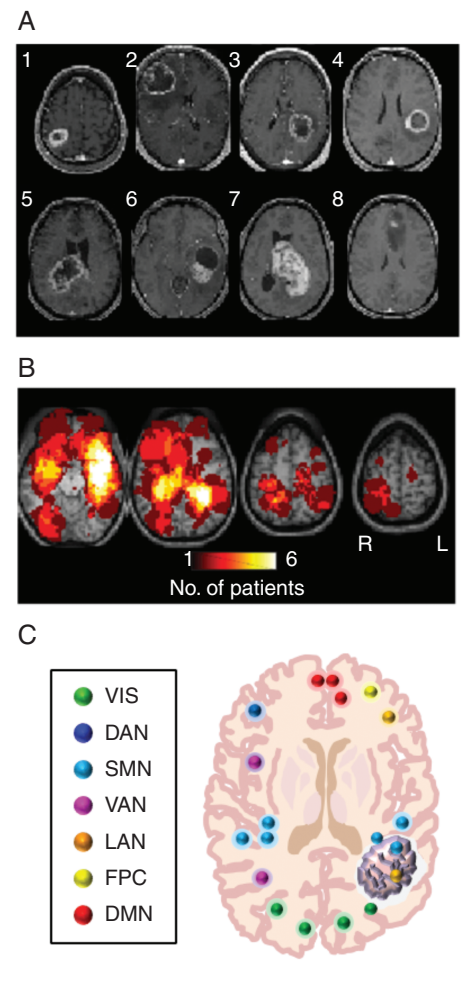
Fig. 1 Intratumor FC in GBM patients. (A) Postcontrast T1w images in a sample of 8 patients. (B) Heatmaps showing the distribution of tumor density in the full sample of 57 patients. (C) Schematic of ROIs used to determine network affiliation. Rs-fMRI time series were averaged over ROIs outside the tumor to define RSN-specific time series. Correlation of these time series against intratumor ROIs yielded assessment of intratumor FC. VIS: visual network; DAN: dorsal attention network; SMN: sensorimotor network; VAN: ventral attention network; LAN: language network; FPC: fronto-parietal control network; DMN: default mode network.

derived via ROIs and voxelwise ($n = 31$). Bonferroni correction was applied to correct for multiple comparisons. Additionally, univariate and multivariate Cox regressions were employed to compare the effects of covariates (age, tumor volume, Karnofsky performance score [KPS], intratumor ROI intranetwork connectivity, intratumor voxelwise network connectivity) on survival. The patients evaluated by Cox regression were isocitrate dehydrogenase (IDH) wild-type ($n = 31$). A P-value of 0.05 indicated statistical significance.

Data and Materials Availability

The GSP data are available at https://www.neuroinfo.org/gsp. Tumor data will be available upon request to E.C.L.

Results

GBM Intratumor Functional Connectivity Is Identifiable in Most Patients

A total of 57 patients (15 females, 42 males) with a histological diagnosis of de novo GBM were retrospectively identified (Table 1). The average age was 57.8 ± 13.9 years (range, 21–83). Most patients had either a partial (*n* = 27) or gross total (*n* = 25) resection followed by chemotherapy and radiation. Heterogeneity of GBM location, size, and morphology is illustrated in Fig. 1A. Fig. 1B shows heatmaps representing the distribution of tumor density (as defined by CE T1w boundaries) in the present patient sample. GBMs were approximately evenly distributed in the left (29 patients) and right (22 patients) hemispheres. Tumor involvement was bilateral in 6 (11%) patients. Genetic studies were performed in most cases (Table 1). These studies included O^6-methylguanine DNA-methyltransferase (MGMT) promoter methylation, IDH1-R132 (IDH1) mutation, and epidermal growth factor receptor (EGFR) amplification.

Table 1 Demographic, clinical, and molecular characteristics of GBM patients

| Summary of Characteristics	
No. of patients	57
Mean age, y (range)	57.8 ± 13.9 (21.4–83.4)
Sex	
Male	42
Female	15
CE volume (cm^3)	39.5 ± 34.9
FLAIR volume (cm^3)	116.0 ± 73.0
KPS, *n* (%)	
>70%	24 (42)
Missing	3
Extent of resection	
Gross total	25
Subtotal	27
Biopsy	1
Laser	4
MGMT status	
Methylated	23
Non-methylated	31
Missing	3
IDH mutation	
Mutated	5
Wild-type	51
Missing	1
EGFR amplification	
Positive	17
Negative	21
Missing	19

Of those whose status was recorded, 23 out of 54 patients (42.6%) showed MGMT methylation; only 5 out of 56 had confirmed IDH1 mutations (8.9%); 17 out of 37 were positive for EGFR amplification (44.7%).

Resting-state time series were extracted from a set of 169 ROIs belonging to 7 canonical RSNs defined in atlas space (Fig. 1C).[24] ROI-based and voxel-based measures were used to evaluate the prevalence and variability of intratumor FC (see Materials and Methods). The patient FC measures were compared with control FC measures derived from 100 normal young adults in the Harvard-MGH Brain GSP dataset.[22] The patient and control data were analyzed identically with "tumor boundaries" in the controls duplicated from those in the patients. Findings using the contralesional mirror site as a control ROI were obtained in a subset of patients (*n* = 35) (see Supplementary Methods and Supplementary Figure 1).

At least one intratumor ROI was found in 93% of GBM patients. Averaging over patients, the mean number of intratumor ROIs per RSN ranged from 0.40 to 2.44. The distribution of intratumor ROI-based FC strengths (Fisher *z*-transformed Pearson correlation) was approximately zero-centered in the patients (Fig. 2A). In contrast, the same quantity in the control population was centered around 0.5 (Fig. 2B). No RSN specificity of intratumor FC was apparent in either group. For all RSNs, the mean "intratumor" FC in the controls was significantly different from zero (one-sample *t*-test, $P < 0.0001$) and significantly different from the corresponding network in GBM patients (two-sample rank sum test, $P < 0.00001$). ROI-based intratumor FC distributions, collapsed over RSNs, are shown in Fig. 2C, D for the patients and controls, respectively. Systematically lower FC in tumor ROIs is expected (GBM patients mean: 0.048 vs 0.52 in controls, unpaired *t*-test, $P < 0.00001$). In principle, FC in nonfunctional tissue should be narrowly distributed about zero (Supplementary Figure 2). Instead, the patient and control distributions were comparably wide, although a small, but statistically significant, difference was found between the FC distribution standard deviations of the patients and controls (GBM patients: 0.24 vs controls: 0.28; *F*-test, $F = 0.7414$, $P < 0.0001$). The mean FC within patient intratumor ROIs was statistically greater than zero (one-sample *t*-test, $P < 0.0001$) with a larger standard deviation than expected by chance (GBM patients: 0.24 vs null distribution: 0.08; *F*-test, $F = 0.1137$, $P < 0.0001$; see Supplementary Figure 2).

The observation of occasionally significant intratumor FC prompted us to investigate the topography of this phenomenon. Six representative patients are illustrated in Fig. 3A. Voxels in which FC with any of the 7 canonical RSNs exceeded 0.3 (operationally defined as "functionally connected") are shown in green. This criterion is arbitrary but provides a basis for comparisons across patients. Functionally connected voxels were very unevenly distributed across patients (Fig. 3B). At least one such voxel was present in 98.3% of patients (*n* = 56). In most patients (*n* = 29), such voxels accounted for less than 20% of the tumor mass. More than half of the tumor mass met this criterion in only 7% of patients (*n* = 4). Functionally connected voxels tended to occur in clusters, but otherwise no characteristic distribution (eg, tumor
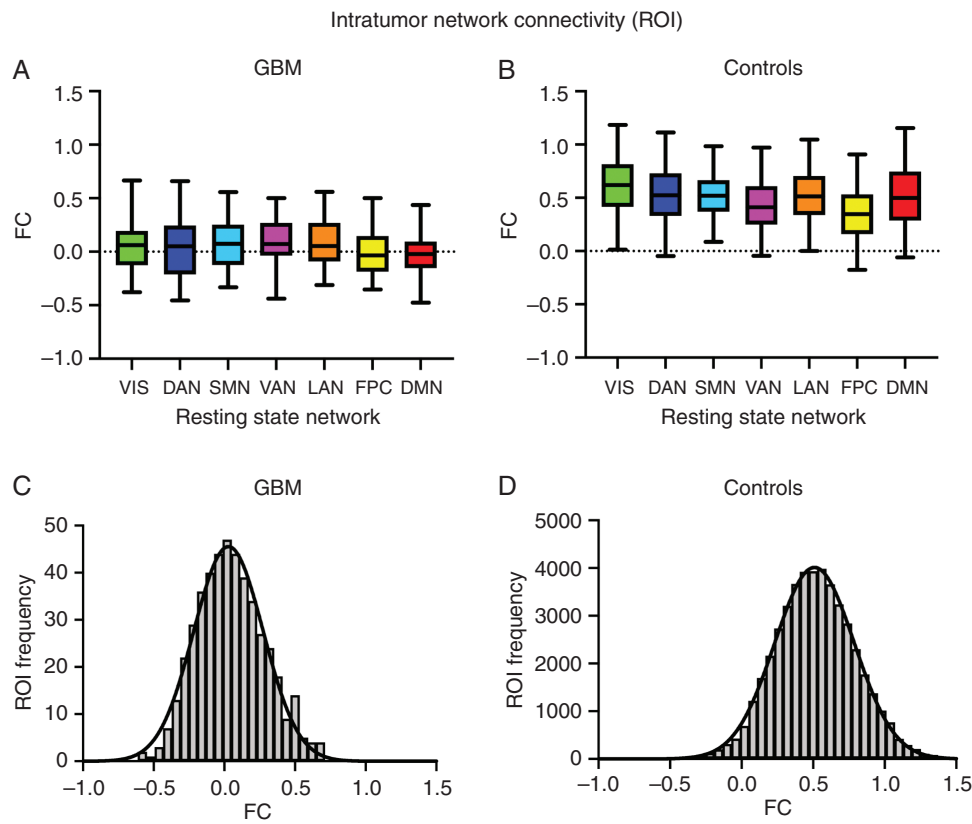
Fig. 2 ROI-based FC (Fisher *z*-transformed correlation) within GBMs. (A) FC in GBM patients (*n* = 53). FC strength is represented as a boxplot corresponding to assigned network. The mean of the VIS, DAN, FPN, and DMN FC distributions were not significantly different from zero (one sample *t*-test, *P* > 0.05). However, in some patients, some ROIs had FC values of 0.5 or greater. (B) Virtual intratumor FC in controls. Each control (*n* = 100) was treated as every GBM patient (*n* = 53) to obtain the expected connectivity strengths and overall intranetwork distributions for the ROIs found within the tumor masks of each GBM patient. The median of every network in controls was greater than its corresponding distribution in GBM patients (two-sample Wilcoxon rank sum-test, *P* < 0.00001). (C) Intratumor FC distribution in GBM patients, collapsed over RSNs. The mean of this distribution is significantly greater than zero (one-sample *t*-test, *P* < 0.0001). (D) Virtual intratumor FC distribution in controls. The mean of this distribution is ~0.5. The control FC distribution is smoother because it represents a larger sample of "intratumor" ROIs.

core vs periphery) was evident on visual inspection. Quantitatively, a greater proportion of functionally connected voxels was found in CE areas compared with necrotic (NEC) regions (CE mean = 0.78 vs NEC mean = 0.22; unpaired *t*-test, *P* < 0.0001; Fig. 3C). The fraction of functionally connected voxels was slightly greater in small versus large tumors (Fig. 3D), although this relation was not statistically significant by formal regression analysis (R^2 = 0.0322, *P* = 0.182).

Strength of GBM Intratumor Functional Connectivity in Relation to Survival

Heterogeneity of intratumor FC across patients raises the possibility that this measure may relate to survival. To examine this possibility, we analyzed the available data in all patients with intratumor ROIs and known survival times (interval between diagnosis and death; *n* = 31; Supplementary Table 1). This analysis was conducted using both ROI-based and voxel-based intratumor FC measures.

In both cases, the patients were median split into low FC and high FC groups, and survival data were compared using the Wilcoxon rank sum test and Kaplan–Meier survival analysis.

The ROI-based FC measure was evaluated as the median intranetwork FC over all intratumor ROIs. Median survival in the high FC group (15.51 mo) was significantly longer than that in the low FC group (8.35 mo) (right-tailed Wilcoxon rank sum, W = 204, *P* < 0.001, Bonferroni corrected) (Fig. 4A). Similarly, Kaplan–Meier analysis demonstrated a significant difference in survival (log-rank test, *P* < 0.001, Bonferroni corrected) (Fig. 4B).

For the voxelwise analysis, each intratumor voxel was assigned a value equal to the maximum FC over the 7 canonical RSNs. The voxel-based FC measure then was evaluated as the median intranetwork FC over all the voxels in each patient's tumor. Median survival times for the high FC and low FC groups were 14.1 months and 10.5 months, respectively. This difference was not significant (right-tailed Wilcoxon rank sum, W = 281, *P* = 0.11, Bonferroni corrected).
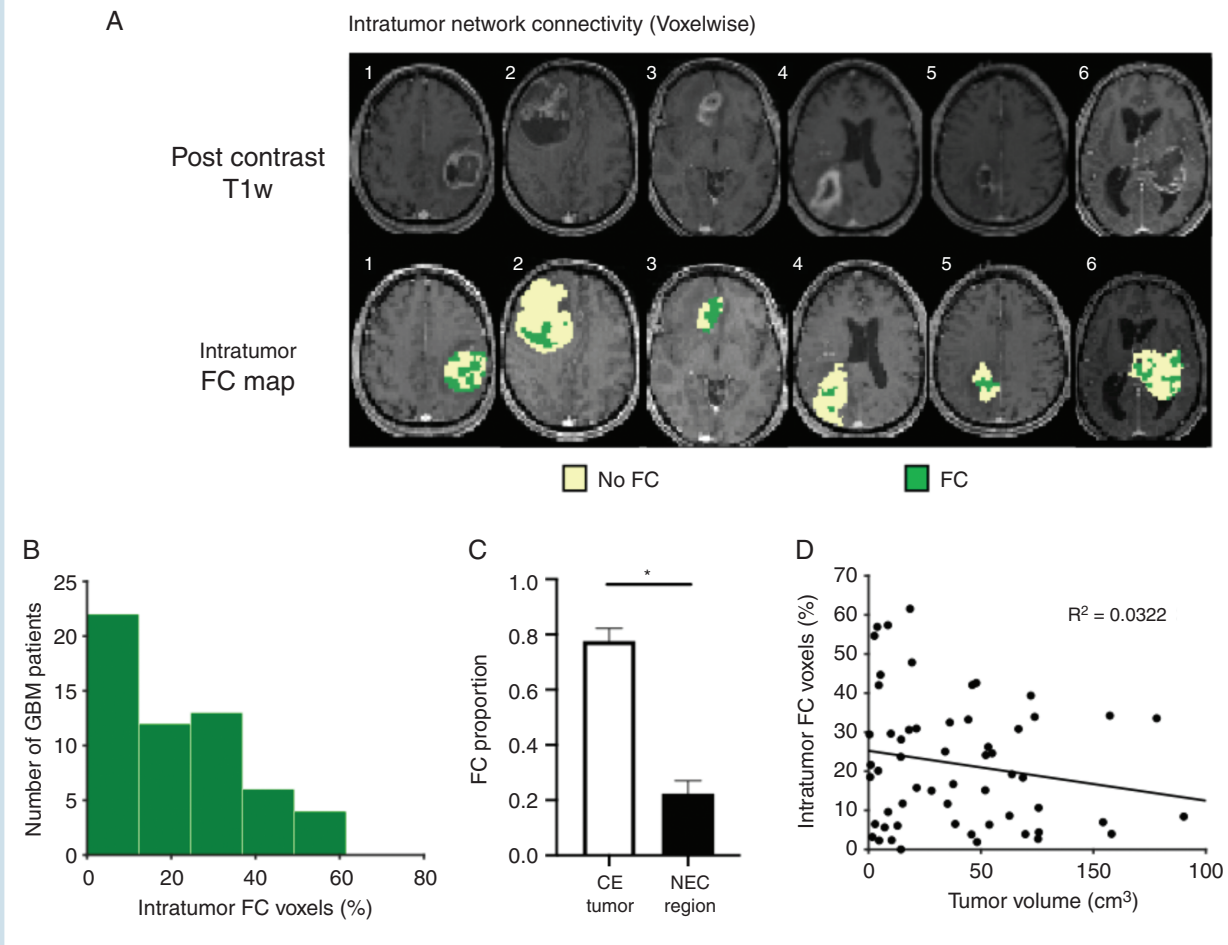
Fig. 3 Voxelwise identification of intratumor function. (A) Postcontrast T1w slices and corresponding intratumor FC maps of 6 GBM patients demonstrate tumor and intratumor FC heterogeneity. Green denotes voxels that were assigned FC after obtaining a correlation $r > 0.3$ with at least one resting-state network. Beige denotes voxels that did not meet this criterion (no FC). (B) Distribution of the percentage of intratumor FC voxels by number of patients reveals that most patients have a low proportion of functional voxels. (C) Bar chart showing the proportion of FC voxels in contrast-enhanced (CE) and necrotic (NEC) areas in GBM tumors ($n = 56$). Error bars denote 95% CI. CE regions demonstrate significantly higher proportion of FC than NEC areas (CE = 0.78 vs NEC = 0.22, unpaired t-test, $P < 0.0001$). (D) Plot of percentage of intratumor FC voxels versus tumor volume demonstrating no significant correlation ($P = 0.182$).

Similarly, the Kaplan–Meier analysis showed a modest difference in survival times (longer survival in the high FC group by log-rank test, $P = 0.084$, Bonferroni corrected) (Fig. 4C).

Multivariate Cox regressions were performed to control for potential influences of clinical and demographic covariates (eg, performance status) on survival times (Table 2). Patients with high postoperative KPS (>70) had longer survival times (hazard ratio [HR]: 0.31, 95% CI: 0.012–0.82, $P = 0.018$), in accordance with previously reported results.[26] The ROI-based FC measure remained prognostic of overall survival after inclusion of demographic covariates (HR: 0.29, 95% CI: 0.12–0.66, $P = 0.0035$). The range of effect sizes was similar for intratumor ROI-based FC and KPS, but intratumor FC was a stronger predictor of survival. Univariate Cox regression showed that intratumor voxelwise FC was a significant predictor of survival, and this effect was maintained with inclusion of age, tumor size, and KPS as covariates (HR: 0.33, 95% CI: 0.13–0.84, $P = 0.021$).

Discussion

It has been reported that functional brain tissue exists within GBM tumors.[3–5] Evidence speaking to this question has so far been limited by functional scope (ie, a focus on eloquent cortex) as well as study parameters (ie, low sample size and heterogeneous tumor pathology). Here, we used rs-fMRI in 57 newly diagnosed GBM patients to non-invasively assess resting state FC within tumor boundaries. Intratumor FC was evaluated in conformity with priors derived from a large sample of normal individuals.[24] Mean FC within tumor boundaries was significantly greater than zero (Fig. 2C, D). Importantly, this measure was remarkably variable over patients (Fig. 3B). Moreover, high intratumor FC was associated with longer survival (Fig. 4).

Some fraction of FC variability is attributable to measurement error.[27] Variable intrinsic activity organization (in
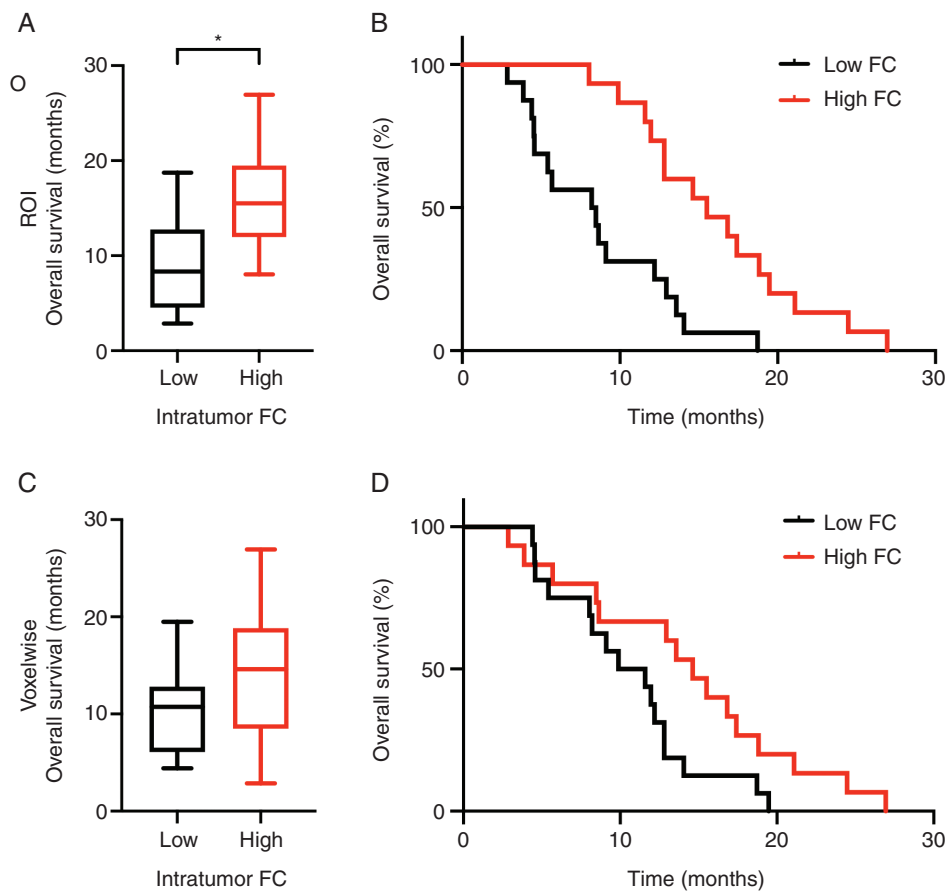
Fig. 4 Intratumor FC stratifies overall survival in GBM patients. (A) ROI derived FC: Overall survival in GBM patients with low intratumor FC are compared with patients with high intratumor FC. Asterisk indicates significant difference (right-tailed Wilcoxon rank sum, W = 240, $P < 0.001$, Bonferroni corrected). (B) ROI derived FC: Kaplan–Meier survival analysis comparing overall survival in low intratumor FC GBM patients and high FC patients. Patients with high intratumor FC had a significantly longer overall survival than those with low intratumor FC (HR: 0.25, 95% CI: 0.11–0.58, $P = 0.0011$). (C) Voxelwise derived FC: Overall survival in GBM patients with low intratumor FC are compared with patients with high intratumor FC (right-tailed Wilcoxon rank sum, W = 281, $P = 0.11$, Bonferroni corrected). (D) Voxelwise derived FC: Kaplan–Meier survival analysis comparing overall survival in low intratumor FC GBM patients and high FC patients. Patients with high intratumor FC had a significantly longer overall survival than those with low intratumor FC (HR: 0.45, 95% CI: 0.21–0.98, $P = 0.044$).

Table 2 Univariate and multivariate survival analysis

Characteristic	Univariate Cox		Multivariate Cox (ROI FC)		Multivariate Cox (voxelwise FC)	
	HR (95% CI)	*P*-value	HR (95% CI)	*P*-value	HR (95% CI)	*P*-value
Age at initial diagnosis	1.01 (0.96,1.05)	0.84	0.996 (0.96, 1.03)	0.79	0.97 (0.93, 1.02)	0.25
CE volume (cm³)	1.02 (1.01,1.03)	**0.0038**	1.02 (1.01, 1.03)	**0.0044**	1.02 (1.01, 1.04)	**0.00095**
KPS > 70	0.33 (0.13, 0.84)	**0.02**	0.31 (0.12, 0.82)	**0.018**	0.35 (0.13, 0.92)	**0.034**
Intratumor FC (ROI) = high	0.25 (0.11,0.58)	**0.0011**	0.29 (0.12, 0.66)	**0.0035**		
Intratumor FC (voxelwise) = high	0.45 (0.21, 0.98)	**0.044**			0.33 (0.13, 0.84)	**0.021**

Cox proportional hazards model was performed for univariate and multivariate regression ($n = 31$).

extratumor tissue) present in all individuals may also contribute.[28,29] Nevertheless, the nearly equal widths of the tumor and control FC distributions is somewhat surprising (Fig. 2C, D, Supplementary Figure 1C, D). Inter-individual differences in the extent of preserved physiology is the most plausible explanation for the finding in question.

The survival results are consistent with this view: tumors with more preserved physiology carry a more favorable prognosis.

GBM tumors characteristically are histologically heterogeneous as well as infiltrative.[31,32] We observed intratumor FC in contrast-enhancing regions as well as hypointense, non-contrast-enhancing regions commonly thought of as necrotic. In principle, FC should not exist within truly necrotic (nonviable) tissue. However, recent work suggests that high cellularity may be present within regions that appear to be necrotic by MRI.[33] Thus, it is plausible that neuropil retaining some degree of FC may be intermixed with nonfunctional tumor cells, as illustrated in Fig. 3A. The low proportion of functionally connected voxels found within necrotic regions also supports this notion (Fig. 3C). Moreover, in our data, the fraction of "functionally connected" voxels was only weakly related to tumor volume (Fig. 3D). This observation also is consistent with the highly infiltrative nature of GBMs.

The survival results shown in Fig. 4 suggest that loss of intratumor FC is a marker of more advanced and/or more aggressive tumors. The simplest explanation for this finding is that tumor growth causes progressive destruction of functioning neural tissue.[2] Alternatively, attenuated FC could result from impaired neurovascular coupling.[34] More elaborate possibilities are suggested by recent work demonstrating that GBM cells form synapses with neurons that interfere with normal excitability and promote invasion.[35,36] The present data cannot distinguish between any of these pathophysiological mechanisms. Thus, although the present results do suggest that retained FC within GBM tumors has positive prognostic value, this observation remains empirical.

A final point that bears discussion is the distinction between evoked versus intrinsic BOLD fMRI signals, the latter of which constitutes the basis of resting-state FC. In the context of presurgical mapping, T-fMRI responses typically appear approximately where expected, outside the tumor (allowing for shifts owing to mass effect) but not inside the lesion; not uncommonly, such responses abruptly truncate at the lesion boundary.[17,37,38] Thus, there would seem to be little reason to expect intrinsic BOLD signal fluctuations inside GBM tumors, notwithstanding that sensory and motor responses to direct electrical stimulation over GBM tumors are well documented.[3,4] The apparent discrepancy between T-fMRI and rs-fMRI is procedural: The objective of T-fMRI is to localize the representation of function outside the tumor with the objective of sparing functional tissue during surgery. In standard practice, no effort is made to detect or display weak T-fMRI responses inside the tumor. Here, in contrast, the analysis is explicitly focused on intratumor voxels, which, on the whole, showed weak evidence of FC with parts of the brain outside the tumor. Statistical analysis revealed that the prevalence of intratumor FC varied widely among patients and this variability carried prognostic value. However, it is unlikely that the "functionally connected" parts of GBM tumors contribute to online behavior. Indeed, we tested this possibility in our patients and found that KPS was unrelated to intratumor FC metrics (both ROI-based and voxel-based), controlling for age and tumor volume (Table 2).

Intratumor FC measures may distinguish patients during the treatment planning phase, enabling neurosurgeons, oncologists, and patients to be more informed prior to surgery. First and foremost, improved prognostication of a given patient's likely outcome following diagnosis would enable the patient to make more informed decisions regarding his/her therapeutic options. As an example, connectivity metrics suggesting a poor prognosis would imply that less aggressive surgery is warranted to preserve function during the limited time the patient has left. Conversely, connectivity metrics suggesting a good prognosis might imply that a more aggressive surgical approach is warranted in order to delay recurrence. These findings may also help in selecting and stratifying patients for clinical trials. However, further studies will be required to evaluate how consistent these findings are in the larger GBM population.

In summary, this study demonstrates that functionally connected brain tissue, as defined by rs-fMRI, is present in the substantial majority of GBM patients. Further, the strength of FC within the tumor has prognostic value. Thus, rs-fMRI as a potential radiological prognostic indicator requires further study.

Supplementary Material

Supplementary data are available at *Neuro-Oncology* online.

Keywords

glioblastoma | glioma | FC | functional MRI | resting state

Conflict of interest statement. A.G.S.D. and E.C.L. have filed a provisional patent on the techniques described in this paper. The authors declare they have no competing interests.

Authorship statement. A.G.S.D., J.S.S., and E.C.L. designed the study; A.G.S.D., J.G., and J.L.R. collected and assembled the data; A.G.S.D., K.Y.P., J.L.R., D.D., J.B.H., C.D.H., and A.Z.S. assisted with the data analysis and interpretation; A.G.S.D., J.S.S., A.Z.S., and E.C.L. wrote the manuscript.

References

1. Wen PY, Kesari S. Malignant gliomas in adults. *N Engl J Med.* 2008;359(5):492–507.
2. Cuddapah VA, Robel S, Watkins S, Sontheimer H. A neurocentric perspective on glioma invasion. *Nat Rev Neurosci.* 2014;15(7):455–465.
3. Ojemann JG, Miller JW, Silbergeld DL. Preserved function in brain invaded by tumor. *Neurosurgery.* 1996;39(2):253–258; discussion 258.
4. Skirboll SS, Ojemann GA, Berger MS, Lettich E, Winn HR. Functional cortex and subcortical white matter located within gliomas. *Neurosurgery.* 1996;38(4):678–684; discussion 684.
5. Schiffbauer H, Ferrari P, Rowley HA, Berger MS, Roberts TP. Functional activity within brain tumors: a magnetic source imaging study. *Neurosurgery.* 2001;49(6):1313–1320; discussion 1320.
6. Sani S, Gerard CS, Byrne RW. Practical application of preoperative and intraoperative cortical mapping in surgery. In: *Functional Mapping of the Cerebral Cortex.* Cham, Switzerland: Springer International Publishing; 2016:159–170.
7. Dallabona M, Sarubbo S, Merler S, et al. Impact of mass effect, tumor location, age, and surgery on the cognitive outcome of patients with high-grade gliomas: a longitudinal study. *Neurooncol Pract.* 2017;4(4):229–240.
8. Campanella F, Shallice T, Ius T, Fabbro F, Skrap M. Impact of brain tumour location on emotion and personality: a voxel-based lesion-symptom mapping study on mentalization processes. *Brain.* 2014;137(Pt 9):2532–2545.
9. Satoer D, Vork J, Visch-Brink E, Smits M, Dirven C, Vincent A. Cognitive functioning early after surgery of gliomas in eloquent areas. *J Neurosurg.* 2012;117(5):831–838.
10. Archibald YM, Lunn D, Ruttan LA, et al. Cognitive functioning in long-term survivors of high-grade glioma. *J Neurosurg.* 1994;80(2):247–253.
11. Brown PD, Ballman KV, Rummans TA, et al. Prospective study of quality of life in adults with newly diagnosed high-grade gliomas. *J Neurooncol.* 2006;76(3):283–291.
12. Lehéricy S, Duffau H, Cornu P, et al. Correspondence between functional magnetic resonance imaging somatotopy and individual brain anatomy of the central region: comparison with intraoperative stimulation in patients with brain tumors. *J Neurosurg.* 2000;92(4):589–598.
13. Lee CC, Ward HA, Sharbrough FW, et al. Assessment of functional MR imaging in neurosurgical planning. *AJNR Am J Neuroradiol.* 1999;20(8):1511–1519.
14. Majos A, Tybor K, Stefańczyk L, Góraj B. Cortical mapping by functional magnetic resonance imaging in patients with brain tumors. *Eur Radiol.* 2005;15(6):1148–1158.
15. Lee MH, Miller-Thomas MM, Benzinger TL, et al. Clinical resting-state fMRI in the preoperative setting: are we ready for prime time? *Top Magn Reson Imaging.* 2016;25(1):11–18.
16. Leuthardt EC, Guzman G, Bandt SK, et al. Integration of resting state functional MRI into clinical practice—a large single institution experience. *PLoS One.* 2018;13(6):e0198349.
17. Rosazza C, Aquino D, D'Incerti L, et al. Preoperative mapping of the sensorimotor cortex: comparative assessment of task-based and resting-state FMRI. *PLoS One.* 2014;9(6):e98860.
18. Raichle ME. The restless brain: how intrinsic activity organizes brain function. *Philos Trans R Soc B Biol Sci.* 2015;370(1668):20140172.
19. Dierker D, Roland JL, Kamran M, et al. Resting-state functional magnetic resonance imaging in presurgical functional mapping sensorimotor localization. *Neuroimag Clin N Am.* 2017;27:621–633.
20. Mitchell TJ, Hacker CD, Breshears JD, et al. A novel data-driven approach to preoperative mapping of functional cortex using resting-state functional magnetic resonance imaging. *Neurosurgery.* 2013;73(6):969–982; discussion 982.
21. Ghinda DC, Wu JS, Duncan NW, Northoff G. How much is enough-Can resting state fMRI provide a demarcation for neurosurgical resection in glioma? *Neurosci Biobehav Rev.* 2018;84:245–261.
22. Yeo BT, Krienen FM, Sepulcre J, et al. The organization of the human cerebral cortex estimated by intrinsic functional connectivity. *J Neurophysiol.* 2011;106(3):1125–1165.
23. Yushkevich PA, Piven J, Hazlett HC, et al. User-guided 3D active contour segmentation of anatomical structures: significantly improved efficiency and reliability. *Neuroimage.* 2006;31(3):1116–1128.
24. Hacker CD, Laumann TO, Szrama NP, et al. Resting state network estimation in individual subjects. *Neuroimage.* 2013;82:616–633.
25. Buckner RL, Sepulcre J, Talukdar T, et al. Cortical hubs revealed by intrinsic functional connectivity: mapping, assessment of stability, and relation to Alzheimer's disease. *J Neurosci.* 2009;29(6):1860–1873.
26. Lamborn KR, Chang SM, Prados MD. Prognostic factors for survival of patients with glioblastoma: recursive partitioning analysis. *Neuro Oncol.* 2004;6(3):227–235.
27. Laumann TO, Snyder AZ, Mitra A, et al. On the stability of BOLD fMRI correlations. *Cereb Cortex.* 2017;27(10):4719–4732.
28. Mueller S, Wang D, Fox MD, et al. Individual variability in functional connectivity architecture of the human brain. *Neuron.* 2013;77(3):586–595.
29. Gordon EM, Laumann TO, Gilmore AW, et al. Precision functional mapping of individual human brains. *Neuron.* 2017;95(4):791–807.e7.
30. Wang D, Liu H. Functional connectivity architecture of the human brain: not all the same. *Neuroscientist.* 2014;20(5):432–438.
31. Brown DV, Stylli SS, Kaye AH, Mantamadiotis T. Multilayered heterogeneity of glioblastoma stem cells: biological and clinical significance. In: *Advances in Experimental Medicine and Biology.* Vol 1139. New York, NY: Springer; 2019:1–21.
32. Catalano M, D'Alessandro G, Trettel F, Limatola C. Role of infiltrating microglia/macrophages in glioma. In: *Advances in Experimental Medicine and Biology.* Vol 1202. New York, NY: Springer; 2020:281–298.
33. Eidel O, Burth S, Neumann JO, et al. Tumor infiltration in enhancing and non-enhancing parts of glioblastoma: a correlation with histopathology. *PLoS One.* 2017;12(1):e0169292.
34. Agarwal S, Sair HI, Pillai JJ. The resting-state functional magnetic resonance imaging regional homogeneity metrics—Kendall's coefficient of concordance-regional homogeneity and coherence-regional

homogeneity—are valid indicators of tumor-related neurovascular uncoupling. *Brain Connect.* 2017;7(4):228–235.

35. Venkatesh HS, Morishita W, Geraghty AC, et al. Electrical and synaptic integration of glioma into neural circuits. *Nature.* 2019:1–7.

36. Venkataramani V, Tanev DI, Strahle C, et al. Glutamatergic synaptic input to glioma cells drives brain tumour progression. *Nature.* 2019:1–8.

37. Schneider FC, Pailler M, Faillenot I, et al. Presurgical assessment of the sensorimotor cortex using resting-state fMRI. *AJNR Am J Neuroradiol.* 2016;37(1):101–107.

38. Håberg A, Kvistad KA, Unsgård G, Haraldseth O. Preoperative blood oxygen level-dependent functional magnetic resonance imaging in patients with primary brain tumors: clinical application and outcome. *Neurosurgery.* 2004;54(4):902–914; discussion 914.

Neuro-
Oncology